Injection of oxygenated Persian Gulf Water into the southern Bay of Bengal

Peter M.F. Sheehan[1], Benjamin G.M. Webber[1,2], Alejandra Sanchez-Franks[3],

Adrian J. Matthews[4], Karen J. Heywood[1] and P.N. Vinayachandran[5]

[1]Centre for Ocean and Atmospheric Sciences, School of Environmental Sciences, University of East Anglia, Norwich, United Kingdom

[2]Climactic Research Unit, University of East Anglia, Norwich, United Kingdom

[3]National Oceanography Centre, Southampton, United Kingdom

[4]Centre for Oceanic and Atmospheric Sciences, School of Environmental Sciences & School of Mathematics, University of East Anglia, Norwich, United Kingdom

[5]Centre for Atmospheric and Oceanic Sciences, Indian Institute of Science, Bangalore, India

Key Points:

- Persian Gulf Water injects oxygen into the Bay of Bengal oxygen minimum zone
- Two transport pathways exist: one in the eastern and one in the western Arabian Sea
- The flux of Persian Gulf Water into the Bay of Bengal is enhanced during the south-west monsoon

Corresponding author: Peter Sheehan, `p.sheehan@uea.ac.uk`

Abstract

Persian Gulf Water (PGW) is an oxygenated, high-salinity water mass that has recently been detected in the Bay of Bengal (BoB). However, little is known about the transport pathways of PGW into the BoB. Ocean glider observations presented here demonstrate the presence of PGW in the southwestern BoB. Output from an ocean re-analysis product shows that this PGW signal is associated with a northward-flowing filament of high-salinity water. Particle tracking experiments reveal two pathways: one in the eastern Arabian Sea that takes a minimum of two years, and another in the western Arabian Sea that takes a minimum of three years. The western pathway connects to the BoB via equatorial currents. The greatest influx of PGW occurs between 82 and 87°E during the southwest monsoon. We propose that injection of PGW to the BoB OMZ contributes to keeping oxygen concentrations in the BoB above the level at which de-nitrification occurs.

Plain-language summary

The Persian Gulf is a hot, shallow sea that acts like a vast salt pan. Consequently, water flowing out of the Gulf has a very high salt concentration; it also has a relatively high dissolved oxygen concentration. This high-salt, high-oxygen signal is distinct to Persian Gulf Water and is largely preserved as Persian Gulf Water spreads in the ocean's interior. In observations collected by an ocean glider, we identify the remnants of this high-salt, high-oxygen signal in the southwestern Bay of Bengal, a region that is notably lacking in dissolved oxygen. Using an ocean model, we identify two pathways taken by Persian Gulf Water between the northern Arabian Sea and the Bay of Bengal: one in the eastern Arabian Sea that takes a minimum of two years; and one in the western Arabian Sea that takes a minimum of three years. Persian Gulf Water arrives in the Bay of Bengal throughout the year, but particularly during the southwest monsoon (June to September). Persian Gulf Water brings oxygen to the Bay of Bengal and potentially plays a role in keeping dissolved oxygen levels in the Bay above the level at which its ecological functioning would be significantly altered.

1 Introduction

Persian Gulf Water (PGW) is an oxygenated, high-salinity water mass that forms in the shallow waters of the Persian Gulf (Figure 1a; Bower, Hunt, & Price, 2000; Prasad,

Ikeda, & Prasanna Kumar, 2001), its high salinity a consequence of the very high evaporation in that region (Prasad et al., 2001; Yao & Johns, 2010). Despite the high degree of mixing that PGW experiences as it passes through the Gulf of Oman and enters the Arabian Sea, this high-salinity, high-oxygen signal is preserved (Figure 1a; Prasad et al., 2001; Vic et al., 2017). PGW is identifiable in the Arabian Sea as a salinity maximum with a density of between 26.2 and 26.8 g kg^{-1} (Jain et al., 2017; Schott & McCreary, 2001) that is distinct from the other high-salinity water masses of the northern Indian Ocean – i.e. Arabian Sea High-Salinity Water (22.8 – 24 kg m^{-3}) and Red Sea Water (27 – 27.4 kg m^{-3}; Jain et al., 2017; Prasanna Kumar & Prasad, 1999). The passage of PGW through the Gulf of Oman and its subsequent spreading in the Arabian Sea are the subject of previous work (e.g. Bower et al., 2000; Ezam, Bidokhti, & Javid, 2010; Prasad et al., 2001; Vic et al., 2017), and the role of PGW in ventilating the Arabian Sea OMZ has been documented (e.g. Lachkar, Lévy, & Smith, 2019; McCreary et al., 2013). The fate of PGW beyond the Arabian Sea has received less attention.

The Bay of Bengal (BoB; Figure 1a) is an oxygen minimum zone (OMZ; D'Asaro, Altaet, Suresh Kumar, & Ravichandran, 2020; McCreary et al., 2013), a region of the ocean where low oxygen concentrations (< 60 μmol kg^{-1}) may be harmful to marine life, and where, when oxygen concentrations are very low (< 6 μmol kg^{-1}), biogeochemical cycles may be significantly altered (Queste, Vic, Heywood, & Piontkovski, 2018). The density range of PGW matches the density range of the BoB OMZ (McCreary et al., 2013). OMZs exert an influence on the nitrogen cycle, and hence on the carbon cycle (Gruber, 2008), that is disproportionate to their size (Johnson, Riser, & Ravichandran, 2019). Understanding the controls on the location, size and functioning of OMZs is therefore of critical importance, particularly as the extent and intensity of OMZs are predicted to increase over the 21st century due to climate change (e.g. Bopp et al., 2013; Oschlies, Schulz, Riebesell, & Schmitter, 2008).

Processes that maintain the BoB OMZ are poorly understood, and it has not been well reproduced in models (McCreary et al., 2013). The strength of stratification in the BoB is such that horizontal oxygen transport from the south is of critical importance (D'Asaro et al., 2020). Johnson et al. (2019) have highlighted the high-degree of variability that dominates the BoB OMZ, and suggest that physical processes resulting in the episodic injection of water with oxygen concentrations between 5 and 10 μmol kg^{-1} keep oxygen concentrations high enough to prevent large-scale denitrification, a chem-

ical process that strips bio-available nitrogen from the water column and thus may hinder phytoplankton growth. Sridevi and Sarma (2020) report that cyclonic and anti-cyclonic eddies can increase and decrease sub-surface oxygen concentrations respectively. Taken together, these results point to a complex relationship between physics and biogeochemistry in the BoB, with oxygen concentrations depending on multiple processes that often operate over small spatial scales. Although the BoB OMZ is weaker than others in which pronounced denitrification occurs (D'Asaro et al., 2020), it may be close to a tipping point: a small reduction in oxygen transport to the OMZ could lead to a large increase in denitrification (D'Asaro et al., 2020; Johnson et al., 2019). Consequently, understanding the flow of oxygenated water masses into the BoB OMZ is essential for understanding both how the BoB OMZ operates today and how it may respond to a changing climate.

Previous studies have disagreed on the presence of PGW in the BoB. Some observational studies have interpreted salinity maxima in the BoB as evidence of PGW (Rochford, 1964; Varadachari, Murty, & Reddy, 1968); others have found no such maxima (Shetye et al., 1993, 1991) or else have found no evidence of PGW beyond the Arabian Sea (Kuksa, 1972; Quadfasel & Schott, 1982; Shenoi, Shetye, D., & Michael, 1993). Modeling studies of PGW either find no transport to the BoB (Han & McCreary, 2001), or else do not address the question (Durgadoo, Rühs, Biastoch, & Böning, 2017). Most recently, Jain et al. (2017) identified PGW in a dozen temperature, salinity and oxygen profiles from across the BoB; they propose that the Southwest Monsoon Current (SMC; Figure 1 Vinayachandran, Masumoto, Mikawa, & Yamagata, 1999; Webber et al., 2018), a relatively strong northeastward flow that occurs during the southwest monsoon (June to September), is the primary conduit for PGW entering the BoB, but pathways from the Persian Gulf to the BoB, and the timescales of transport, have not been identified. Here, we present a case study of PGW injection into the BoB, from which we determine transport pathways and timescales from the northern Arabian Sea to the BoB. We use ocean glider observations and 11 years of output from a NEMO ocean reanalysis to examine the injection of PGW into the BoB, and to place our case study into an interannual context. We propose that the episodic injection of trace amounts of PGW into the BoB acts to ventilate the BoB OMZ and provide the first estimates of the amount of oxygen that PGW may supply to the BoB OMZ.

2 Glider observations of Persian Gulf Water in the Bay of Bengal

Observations were collected using an ocean glider in the southwestern BoB (8°N, 85.4°E) in July 2016 as part of the Bay of Bengal Boundary Layer Experiment (BoB-BLE; Figure 1a; Vinayachandran et al., 2018; Webber et al., 2018). PGW is observed as a salinity maximum between the 26.2 and 26.8 kg m^{-3} isopycnals (Figure 1b and c), corresponding to depths between approximately 200 and 250 m. The salinity maximum exhibits elevated oxygen concentrations (Figure 1b and c): up to 30 μmol kg^{-1}, against a background concentration between the 26.2 and 26.8 kg m^{-1} isopycnals of below 10 μmol kg^{-1}. The oxygen concentration of PGW in the BoB is greatly decreased compared to its oxygen concentration in the Gulf of Oman (approximately 100 μmol kg^{-1}; Queste et al., 2018), close to its source region, presumably due to mixing with lower-oxygen water masses and biological oxygen consumption. The oxygen sensor malfunctioned approximately halfway through the deployment; temperature and salinity observations without an associated oxygen observations are plotted in gray in Figure 1b and c).

The salinity maximum and elevated oxygen concentration are indicative of the presence of PGW. There is a strong link between absolute salinity and oxygen concentration within the PGW density layer: stronger salinity maxima are associated with higher oxygen concentrations (Figure 1b and c). The background water mass between 26.2 and 26.8 kg m^{-1} in this region is North Indian Central Water (You, 1997), which is typified by low oxygen concentrations. PGW entering the BoB thus increases the oxygen concentration and is likely to be the only source of relatively oxygenated waters for the BoB OMZ between these isopycnals. PGW was not observed by any of the four other BoB-BLE gliders deployed contemporaneously further east along 8°N (not shown; Vinayachandran et al., 2018), which suggests that the inflow was of limited horizontal extent.

PGW may be identified in temperature-salinity space as saline deviations from the background temperature-salinity curve (Figure 1b and c). Whereas previous work has identified a tendency towards higher salinities within the range of PGW densities (Jain et al., 2017), our observations reveal a pronounced and sharply defined local salinity maximum indicative of a PGW layer that is distinct from the layers immediately above and below.

3 Pathways and timescales of Persian Gulf Water transport to the Bay of Bengal

Pathways and timescales of transport between the Persian Gulf and the BoB are investigated using the Nucleus for European Modelling of the Ocean (NEMO) version 3.1 (Madec, 2008) ocean re-analysis. A salinity maximum on the 26.5 kg m^{-3} isopycnal at the time and location of the glider observations is identified in the NEMO output; this closely resembles the signal of PGW found in the glider observations (Figure 1b and c).

Salinity and velocity are linearly interpolated in density space onto the 26.5 kg m^{-3} isopycnal; this isopycnal has previously been taken as the core density of PGW (Bower et al., 2000; Prasad et al., 2001). The salinity maximum is associated with a filament of high-salinity (> 35.25 g kg^{-1}) water flowing northeastward from the saline waters found south of 4°N to the relatively fresher waters of the BoB (Figure 2). We take this filament to be the feature associated with the PGW intrusion found in our observations. The filament, which is located on the western flank of the SMC and is apparent over a period of approximately one month, evolves in time, extending progressively further northward into the southern BoB, before being caught between a cyclonic eddy to the north and an anti-cyclonic eddy to the south. The filament eventually splits, with the northern part continuing to be advected north (Figure 2). The presence of the filament also demonstrates that PGW advection into the BoB may happen as part of sporadic physical structures rather than being a diffuse phenomenon.

We perform backward-trajectory particle tracking experiments to determine the transport pathways and timescales of water in the filament. We follow the method of Sanchez-Franks et al. (2019). Model velocities on the 26.5 kg m^{-3} isopycnal are bi-linearly interpolated to the particle locations, and the particles are advected using a fourth-order Runge-Kutta scheme with a time step of 12 hours. We assume that diapycnal diffusivity is negligible and that PGW remains at the 26.5 kg m^{-3} isopycnal. Particles are released daily between 24 June and 8 July 2016 inclusive, in a grid pattern at 1 km intervals between 6 and 7°N, and 84 and 86°E (Figure 2b). Not all grid points fall within the plume on all days. A total of 374,640 particles are released and are tracked backwards in time for five years (i.e. to July 2011). Any particle that is found to have a source region north of 20°N in the Arabian Sea is taken to be indicative of PGW transport to the BoB. Note that by source region we refer to the end point of the backward trajectory – that is, the start point of the equivalent forward trajectory. North of 20°N, PGW occupies the en-

176   tire Arabian Sea on the 26.5 kg m^{-3} isopycnal (Prasad et al., 2001; Shenoi et al., 1993).

177   We do not attempt to track particles back to the Persian Gulf, because the complex eddy-

178   topography interactions that occur as PGW exits the Persian Gulf lead to significant di-

179   apycnal mixing in this region (Bower et al., 2000; Vic et al., 2017).

180   Of the backwards-tracked particles, 643 (0.17%) have a source region in the north-

181   ern Arabian Sea. This is consistent with the small volume of PGW observed in the BoB.

182   Two main pathways are identified along which PGW is advected (*forward* in time) from

183   the northern Arabian Sea to the southern BoB (Figure 3b). Following the eastern path-

184   way (*forward* in time), PGW is transported southward along the coast of India, then is

185   transported eastward to the south of Sri Lanka, before entering the BoB (Figure 3b). Fol-

186   lowing the western pathway (*forward* in time), PGW is transported southward along the

187   coasts of Oman and Somalia before turning eastward north of the equator. South of In-

188   dia, at approximately 75°E, it joins up with PGW following the eastern pathway and

189   is similarly transported into the BoB (Figure 3b). These pathways, particularly the west-

190   ern pathway, resemble those identified by Sanchez-Franks et al. (2019) for the transport

191   of Arabian Sea High-Salinity Water to the BoB. This is the first time that the spread-

192   ing of PGW along both sides of the Arabian Sea has been linked to transport to the BoB.

193   All these particle trajectories converge into the SMC; this is to be expected since the par-

194   ticles were released in a plume associated with this current.

195   To determine whether the salinity of the water masses observed align with their

196   source region, we associate each particle with the salinity at the release point of its back-

197   ward trajectory (Figure 2b), interpolated from NEMO data. The mean salinity of par-

198   ticles that have a source region in the northern Arabian Sea (35.30 g kg^{-1}) is higher than

199   that of particles that have a source region elsewhere (35.16 g kg^{-1}; Figure 3a) and is higher

200   than the 35.25 g kg^{-1} threshold used previously to define the high-salinity filament (Fig-

201   ure 2). The mean salinity of particles that have a source region in the northern Arabian

202   Sea cannot be reproduced by random Monte Carlo sampling (n = 1,000,000) of the salin-

203   ity distribution of all released particles. Hence, the particles that have a source region

204   in the northern Arabian Sea are extremely unlikely (p < 0.001) to be the result of ran-

205   dom sampling.

206   Using 11 years of NEMO re-analysis (January 2007 to December 2017 inclusive),

207   we perform a forward-trajectory particle tracking experiment to test whether the advec-

tion of PGW from the northern Arabian Sea to the BoB is a persistent phenomenon. Particles are released on the first day of every month between January 2007 and December 2012 along a transect at 20°N, from the eastern coast of Oman (58°E) to the western coast of India (72°E). Any particle that crosses 8°N between the eastern coast of Sri Lanka and 98°E is considered to be indicative of PGW transport to the BoB. Of the forwards-tracked particles, 0.025% reach the BoB. This indicates that a very small fraction of PGW is transported into the BoB on these time scales. However, even the low concentrations observed here can raise the oxygen concentration on arrival in the BoB (Figure 1b and c). The eastern and western pathways identified in the case study also emerge from the forward trajectories (Figure 3c). The majority (84%) of particles follow the eastern pathway, which suggests that the more equal separation between eastern and western pathways found for the July 2016 filament was unusual.

The first PGW particles in the forward-trajectory experiment arrive in the BoB via the eastern pathway between 1.5 and two years after being released in the northern Arabian Sea (blue colors in Figure 4a); the first particles arrive via the western pathway just under three years after being released (orange colors Figure 4a). The flux of PGW particles into the BoB reaches a maximum between four and five years after release (Figure 4a). The flux of PGW into the BoB is enhanced between May and September (Figure 4b) – that is, during the southwest monsoon. The influence of this enhancement is seen in the distribution of transport times, being responsible for local peaks in transport time that occur approximately one year apart. The diagonal colored lines in Figure 4a connect transport times that result in particles being advected northwards across 8°N during the same southwest monsoon season; the distribution of transport time is better explained by month of entry than by month of release.

The range of longitudes at which the majority of these particles enter the BoB during the southwest monsoon, i.e. between 82 and 87°E (Figure 4b), is consistent with the location of the SMC (Figure 1; Vinayachandran et al., 1999), suggesting that the SMC is the primary feature responsible for advecting PGW into the BoB. The SMC is a surface-intensified current – greatest flow speeds are found in the top 150 m – but climatological mean northward flow extends to approximately 400 m (Webber et al., 2018). SG579 was placed in the eastern portion of this PGW flux region (Figures 1a and 4b). Four other gliders deployed during the BoBBLE campaign were located between 87 and 89°E, at which longitudes relatively fewer PGW particles enter the BoB (Figure 4b); this suggests

that the lack of PGW to the east of SG579 was not atypical. Our finding that the SMC is largely responsible for the advection of PGW into the BoB agrees with the hypothesis of Jain et al. (2017), but our results also demonstrate that small amounts of PGW enter the BoB at other times of year and at other longitudes, most notably in December (Figure 4b).

We hypothesise that the transport of PGW between the northern Arabian Sea and the BoB, and the dominance of the eastern pathway, may be explained by the effect of the seasonally reversing currents of the northern Indian Ocean on interannual timescales. Southward flow via the eastern pathway at the depth of the 26.5 kg m^{-3} isopycnal occurs during the northeast monsoon in an undercurrent associated with the West India Coastal Current (WICC; Amol et al., 2014); the WICC itself is too shallow (top 100 m) to affect the 26.5 kg m^{-3} isopycnal. The annual cycle of flow in this undercurrent is six months out of phase with flow in the WICC, being northward during the southwest monsoon and southward during the northeast monsoon (Amol et al., 2014). Despite these semi-annual flow reversals, annual mean flow is southward (Amol et al., 2014). Consequently, PGW entrained in this undercurrent, which stretches the full width of the western coast of India (Amol et al., 2014), will be advected southward. That the majority of PGW particles follow this eastern pathway is probably because it represents a more direct route to the BoB. Particles that follow the western pathway in the Arabian Sea are more likely to be advected to other parts of the ocean – for instance the southern Indian Ocean (Durgadoo et al., 2017).

4 Influence of Persian Gulf Water on the Bay of Bengal oxygen minimum zone

Oxygenated PGW entering the BoB throughout the year supports the hypothesis proposed by McCreary et al. (2013) and Johnson et al. (2019): that the BoB OMZ is kept at oxygen concentrations above the level at which denitrification occurs by physical processes that sporadically inject relatively oxygenated water. Johnson et al. (2019) propose that eddies are primarily responsible for this flux of oxygenated water, and note that eddies have previously been identified as key transporters of oxygen into other OMZs (e.g. Lachkar, Smith, Lévy, & Pauluis, 2016; Resplandy et al., 2012). The flux of PGW identified here could be a physical process responsible for the ventilation of the BoB OMZ. Johnson et al. (2019) find no seasonality in the BoB OMZ, and it is plausible that the

273 effect of the seasonal enhancement in the PGW flux driven by the SMC is diminished

274 as PGW is re-distributed and its oxygen consumed.

275 We perform an idealised calculation to produce an order-of-magnitude estimate of

276 the amount of oxygen, ΔO_{PGW}, supplied to the BoB OMZ by the filament identified in

277 this study (Figures 1 and 2). We consider a filament that contains PGW and lower-oxygen

278 ambient water. The mass of the filament, M_{FIL}, is given by:

$$M_{FIL} = W \times H \times U \times \Delta t \times \rho, \tag{1}$$

279 where $W = 100$ km is the width of the high-salinity filament (Figure 2), $H = 100$ m is

280 its vertical extent (from glider observations; not shown), $U = 0.2$ m s^{-1} is its speed (Fig-

281 ure 2), $\Delta t = 15$ days is its duration (from NEMO re-analysis; not shown) and $\rho = 1026.5$ kg m^{-3}

282 is its density (Figure 1). This gives $M_{FIL} = 2.7 \times 10^{15}$ kg. For PGW with an oxygen

283 concentration of 20 μmol kg^{-1} (Figure 1c) and ambient water with an oxygen concen-

284 tration of 10 μmol kg^{-1} (Figure 1c; D'Asaro et al., 2020), PGW provides additional oxy-

285 gen at 10 μmol kg^{-1}. Multiplied by mass M_{FIL}, this equates to $\Delta O_{PGW} = 2.7 \times 10^{16}$ μmol.

286 The increase in oxygen concentration effected by ΔO_{PGW} depends on the volume

287 over which it is re-distributed; if re-distributed over the mass of the entire BoB OMZ,

288 M_{OMZ} (we assume 1,000 by 1,000 km by 400 m, therefore $M_{OMZ} = 4.1 \times 10^{17}$ kg),

289 the increase in oxygen concentration resulting from ΔO_{PGW} of this filament would be

290 0.07 μmol kg^{-1}. In more general terms, the additional oxygen supplied by any such fil-

291 ament is diluted by a factor of $M_{OMZ}/M_{FIL} \approx 150$. However, Johnson et al. (2019)

292 propose that the BoB OMZ is characterised by its variability rather than its mean state,

293 and conclude that small changes to the mean state are of limited importance given the

294 dominance of variability. Consequently ΔO_{PGW} need not be spread over the entire vol-

295 ume of the BoB OMZ in order to be of biogeochemical significance; in our idealised cal-

296 culation, this reduces both M_{OMZ} and the dilution factor.

297 Speculating on the volume of the OMZ that is influenced by ΔO_{PGW} is, at present,

298 necessarily subjective, and a thorough treatment of this question is beyond the scope of

299 this study. But we note that, Jain et al. (2017) find no evidence of elevated oxygen within

300 the PGW density range in northern and eastern parts of the BoB. Consequently, we first

301 assume that PGW is re-distributed over the southwestern corner of the BoB OMZ (500

by 500 km). Second, we assume that diapycnal mixing is negligible compared with isopycnal mixing, and the input of ΔO_{PGW} thus retains its original vertical extent (i.e. 100 m). ΔO_{PGW} would therefore be re-distributed over a mass of 2.6×10^{16} kg and would raise the oxygen concentration by 1 μmol kg^{-1} – i.e. by 20% of the background concentration in this region (D'Asaro et al., 2020). If additional PGW flux events occur throughout the year (Figure 4b), our figures will be an underestimate of the influence of PGW on the BoB OMZ over a year. The oxygen profile from the SMC region (recorded during the southwest monsoon of 2012) presented by Jain et al. (2017) exhibits a peak of approximately 30 μmol kg^{-1} within the PGW density range, suggesting that the PGW-containing high-salinity filament we have presented (Figures 1 and 2), and the attendant oxygen flux we have considered in this section, are not isolated events. Further research is necessary to accurately quantify the influence of oxygenated PGW on the BoB OMZ.

5 Conclusions

We have presented observations of a coherent inflow of PGW into the southern BoB. The flow occurs between the 26.2 and 26.8 kg m^{-3} isopycnals and exhibits the elevated salinity and oxygen concentration that are characteristic of PGW (Bower et al., 2000; McCreary et al., 2013; Prasad et al., 2001; Queste et al., 2018). Other water masses between these isopycnals lack the elevated oxygen concentrations of PGW (You, 1997), suggesting that PGW is likely the only means by which the BoB OMZ may be ventilated between these isopycnals.

The inflow is present in the NEMO ocean reanalysis as a filament of high-salinity water flowing from the region of high-salinity (> 35.25 g kg^{-1}) water close to the equator on 26.5kg m^{-3} into the fresher waters of the southern BoB. Particle tracking experiments demonstrate that PGW is transported to the BoB principally via the West India Coastal Current in the eastern Arabian Sea, but also via the western Arabian Sea and via equatorial currents. Both spreading pathways connect the northern Arabian Sea to the southern BoB on timescales of longer than two years. Our results reveal a year-round flux of PGW into the BoB that is enhanced during the southwest monsoon. The location of this flux, which is predominantly between 82 and 87°E, matches the location of the SMC, a strong current that flows northward in the BoB at this time.

Recent work has focused attention on the highly variable oxygen concentrations in its OMZ and, in contrast to the Arabian Sea, suggests a system dominated by this variability (Johnson et al., 2019). The sporadic injection of PGW into the BoB OMZ, and the associated oxygen supply, has the potential to cause marked local elevations in oxygen concentration and, as such, should be considered alongside features such as eddies in future studies of the BoB OMZ. From our observations, we estimate that PGW may deliver approximately 20% of the oxygen in the southwestern BoB OMZ. The PGW layer is predicted to shoal under climate change, as warming of the Gulf increases PGW's core temperature (Lachkar et al., 2019). Any such warming could alter the depth at which PGW enters the BoB, and so reduce ventilation of the BoB OMZ. Given the proximity of the BoB OMZ to the denitrification threshold, any reduction in oxygen could have profound consequences for the biogeochemical and ecological functioning of the BoB and for the global nitrogen cycle.

Acknowledgments

References

Amol, P., Shankar, D., Fernando, V., Mukherjee, A., Aparna, S. G., Fernandes, R., . . . Vernekar, S. P. (2014). Observed intraseasonal and seasonal variability of the West India Coastal Current on the continental slope. *Journal of Earth System Science*, *123*, 1045 − 1074.

Bopp, L., Resplandy, L., Orr, J. C., Doney, S. C., Dunne, J. P., Gehlen, M., . . . Vichi, M. (2013). Multiple stressors of ocean ecosystems in the 21st century: projections with CMIP5 models. *Biogeosciences*, *10*, 6255 − 6245.

363 Bower, A. S., Hunt, H. D., & Price, J. F. (2000). Character and dynamics of the Red Sea

364   and Persian Gulf outflows. *Journal of Geophysical Research*, *105*, 6387 – 6414.

365 D'Asaro, E., Altaet, M., Suresh Kumar, N., & Ravichandran, M. (2020). Structure of the

366   Bay of Bengal oxygen deficient zone. *Deep-Sea Research II*,

367   doi.org/10.1016/j.dsr2.2019.104650.

368 Durgadoo, J. V., Rühs, S., Biastoch, A., & Böning, C. W. B. (2017). Indian Ocean

369   sources of Agulhus leakage. *Journal of Geophysical Research: Oceans*, *122*,

370   3481 – 3499.

371 Ezam, M., Bidokhti, A. A., & Javid, A. H. (2010). Numerical simulations of spreading of

372   the Persian Gulf outflow into the Oman Sea. *Ocean Science*, *6*, 887 – 900.

373 Gruber, N. (2008). The marine nitrogen cycle: overview and challenges. In D. G. Capone,

374   D. A. Bronk, M. R. Mulholland, & E. J. Carpenter (Eds.), *Nitrogen in the marine*

375   *environment* (pp. 1 – 50). Burlington, United States of America.

376 Han, W., & McCreary, J. P. (2001). Modelling salinity distributions in the Indian Ocean.

377   *Journal of Geophysical Research*, *106*, 859 – 877.

378 Jain, V., Shankar, D., Vinayachandran, P. N., Kankonkar, A., Chatterjee, A., Amol, P.,

379   … Neema, C. P. (2017). Evidence for the existence of Persian Gulf Water and Red

380   Sea Water in the Bay of Bengal. *Climate Dynamics*, *48*, 3207 – 3226.

381 Johnson, K. S., Riser, S. C., & Ravichandran, M. (2019). Oxygen variability controls

382   denitrification in the Bay of Bengal oxygen minimum zone. *Geophysical Research*

383   *Letters*, *46*, 804 – 811.

384 Kuksa, V. I. (1972). Some peculiarities of the formation and distribution of intermediate

385   layers in the Indian Ocean. *Oceanology*, *12*, 21 – 30.

386 Lachkar, Z., Lévy, M., & Smith, S. (2019). Strong intensification of the Arabian Sea

387   oxygen minimum zone in response to Arabian Gulf warming. *Geophysical Research*

388   *Letters*, *46*, 5420 – 5429.

389 Lachkar, Z., Smith, S., Lévy, M., & Pauluis, O. (2016). Eddies reduce denitrification and

390   compress habitats in the Arabian Sea. *Geophysical Research Letters*, *43*,

391   9148 – 9156.

392 Madec, G. (2008). *NEMO ocean engine. Note du Pôle de modélisation* (Tech. Rep. No.

393   27. ISSN no 1288-1619). France: Institute Pierre-Simon Laplace.

394 McCreary, J. P., Z., Y., Hood, R. R., Vinayachandran, P. N., Furue, R., Ishida, A., &

395   Richards, K. J. (2013). Dynamics of the Indian Ocean oxygen minimum zones.

Progress in Oceanography, *112-113*, 15 – 37.

Oschlies, A., Schulz, K. G., Riebesell, U., & Schmitter, A. (2008). Simulated 21st century's increase in oceanic suboxia by CO_2-enhanced biotic carbon export. *Global Biogeochemical Cycles*, *22*, GB4008.

Prasad, T. G., Ikeda, M., & Prasanna Kumar, S. (2001). Seasonal spreading of the Persian Gulf water mass in the Arabian Sea. *Journal of Geophysical Research*, *106*, 17059 – 17071.

Prasanna Kumar, S., & Prasad, T. G. (1999). Formation and spreading of Arabian Sea high-salinity water mass. *Journal of Geophysical Research*, *104*, 1455 – 1464.

Quadfasel, D., & Schott, F. (1982). Water mass distributions at intermediate layers off the Somali coast during the onset of the southwest monsoon. *Journal of Physical Oceanography*, *12*, 1358 – 1372.

Queste, B. Y., Vic, C., Heywood, K. J., & Piontkovski, S. A. (2018). Physical controls on oxygen distribution and denitrification potential in the northwest Arabian Sea. *Geophysical Research Letters*, *45*, 4143 – 4152.

Resplandy, L., Lévy, M., Bopp, L., Echevin, V., Pous, Sarma, V. V. S. S., & Kumar, D. (2012). Controlling factors of the oxygen balance in the Arabian Sea's OMZ. *Biogeosciences*, *9*, 5095 – 5109.

Rochford, D. J. (1964). Salinity maxima in the upper 1000 metres of the North Indian Ocean. *Australian Journal of Marine and Freshwater Research*, *15*, 1 – 24.

Sanchez-Franks, A., Webber, B. G. M., King, B. A., Vinayachandran, P. N., Matthews, A. J., Sheehan, P. M. F., . . . Neema, C. P. (2019). The railroad switch effect of seasonally reversing currents on the Bay of Bengal high-salinity core. *Geophysical Research Letters*, *46*, 6005 – 6014.

Schott, F. A., & McCreary, J. P. (2001). The monsoon circulation of the Indian Ocean. *Progress in Oceanography*, *51*, 1 – 123.

Shenoi, S. S. C., Shetye, S. R., D., G. A., & Michael, G. S. (1993). Salinity extrema in the Arabian Sea. In V. Ittekkot & R. R. Nair (Eds.), *Monsoon Biogeochemsitry* (pp. 37 – 49). Hamburg, Germany: University of Hamburg.

Shetye, S. R., D., G. A., Shenoi, S. S. C., Sundar, D., Michael, G. S., & Nampoothiri, G. (1993). The western boundary current of the seasonal subtropical gyre in the Bay of Bengal. *Journal of Geophysical Research*, *98*, 945 – 954.

Shetye, S. R., Shenoi, S. S. C., D., G. A., Michael, G. S., Sundar, D., & Nampoothiri, G.

429 (1991). Wind-driven coastal upwelling along the western boundary of the Bay of

430 Bengal during the southwest monsoon. *Continental Shelf Research*, *11*, 1397 – 1408.

431

432 Sridevi, B., & Sarma, V. V. S. S. (2020). A revist to the regulation of the oxygen

433 minimum zone in the Bay of Bengal. *Journal of Earth System Science*, *129*, 107.

434 Varadachari, V. V. R., Murty, C. S., & Reddy, C. V. G. (1968). Salinity maxima

435 associated with some sub-surface water masses in the upper layers of the Bay of

436 Bengal. *Bulletin of the National Institute of Sciences of India*, *38*, 338 – 343.

437 Vic, C., Roullet, G., Capet, X., Carton, X., Molemaker, M. J., & Gula, J. (2017).

438 Eddy-topography interactions and the fate of the Persian Gulf outflow. *Journal of*

439 *Geophysical Research: Oceans*, *120*, 6700 – 6717.

440 Vinayachandran, P. N., Masumoto, Y., Mikawa, T., & Yamagata, T. (1999). Intrusion of

441 the Southwest Monsoon Current into the Bay of Bengal. *Journal of Geophysical*

442 *Research*, *104*, 11077 – 11085.

443 Vinayachandran, P. N., Matthews, A. J., Vijay Kumar, K., Sanchez-Franks, A., Thushara,

444 V., George, J., . . . Joshi, M. (2018). BoBBLE (Bay of Bengal Boundary Layer

445 Experiment): ocean-atmosphere interaction and its impact of the South Asian

446 monsoon. *Bulletin of the American Meteorological Society*, *99*, 1569 – 1587.

447 Webber, B. G. M., Matthews, A. J., Queste, B. Y., Lee, G. A., Cobas-Garcia, M.,

448 Heywood, K. J., & Vinayachandran, P. N. (2019). Ocean glider data from five

449 Seagliders deployed in the Bay of Bengal during the BoBBLE (Bay of Bengal

450 Boundary Layer Experiment) project in July 2016. *British Oceanographic Data*

451 *Centre, National Oceanography Centre, NERC, DOI: doi:10/dgvj*.

452 Webber, B. G. M., Matthews, A. J., Vinayachandran, P. N., Neema, C. P.,

453 Sanchez-Franks, A., Vijith, V., . . . Baranowski, D. B. (2018). The dynamics of the

454 Southwest Monsoon Current in 2016 from high-resolution observations and models.

455 *Journal of Physical Oceanography*, *48*, 2259 – 2282.

456 Yao, F., & Johns, W. E. (2010). A HYCOM modelling study of the Persian Gulf: 2.

457 formation and export of Persian Gulf Water. *Journal of Geophysical Research*, *115*,

458 C11018.

459 You, Y. (1997). Seasonal variations of thermocline circulation and ventilation in the

460 Indian Ocean. *Journal of Geophysical Research*, *102*, 10391 – 10422.
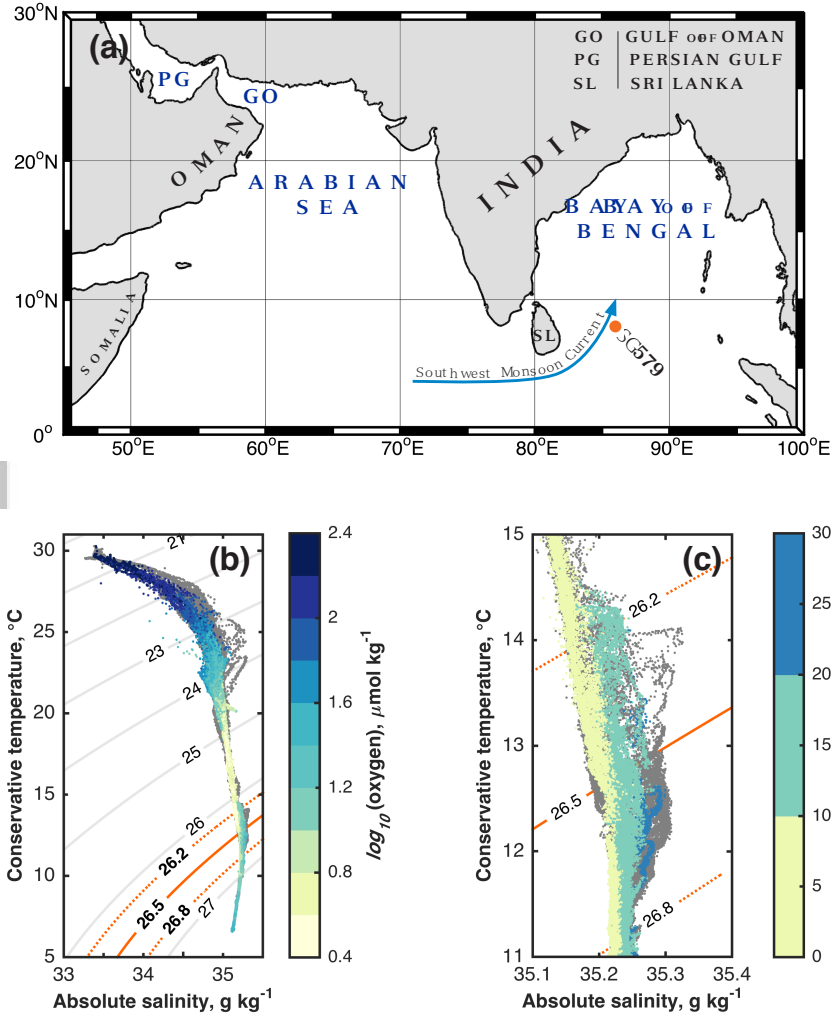
Figure 1. **(a)** Map of the northern Indian Ocean, showing the location of Seaglider (SG) 579. The approximate path of the Southwest Monsoon Current (Vinayachandran et al., 1999) is shown by the blue arrow. **(b)** Temperature-salinity plot of glider observations colored by the logarithm of oxygen concentration (μmol kg^{-1}). **(c)** As panel (b), but zoomed-in to the Persian Gulf Water density range, and colored by oxygen concentration (μmol kg^{-1}). The oxygen sensor was not operational for all dives: gray dots indicate temperature and salinity observations that lack a corresponding oxygen observation.
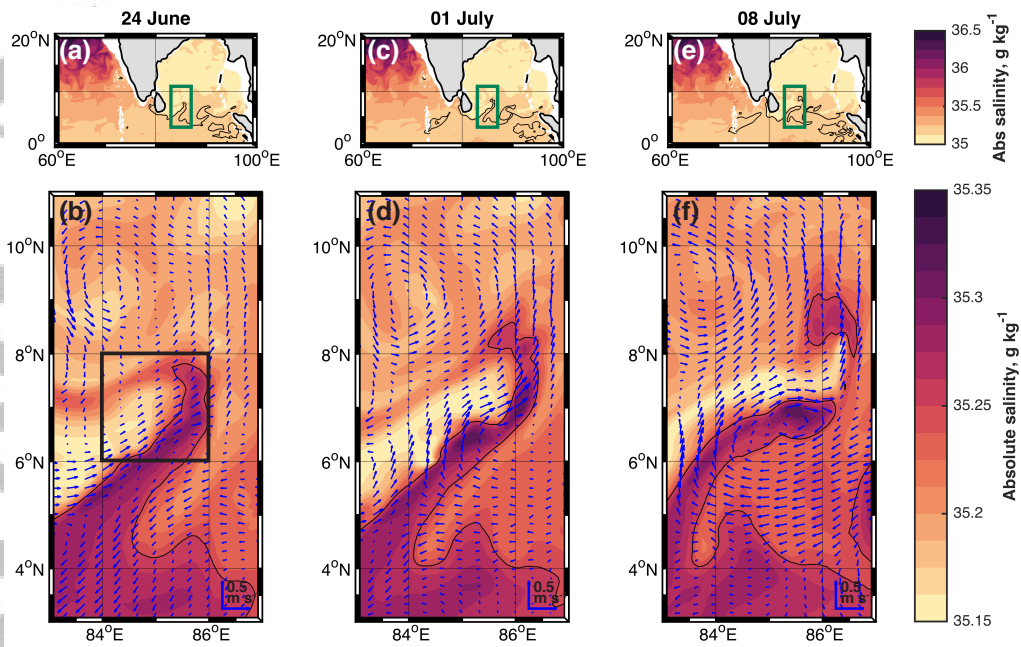
Figure 2. Absolute salinity on the 26.5 kg m^{-3} density surface in the NEMO re-analysis on (**a**) and (**b**) 24 June, (**c**) and (**d**) 1 July, (**e**) and (**f**) 8 July 2016. The area mapped in the bottom panels is indicated by the green boxes in the top panels. The 35.25 g kg^{-1} isohaline is indicated by the black contour in all panels. Arrows indicate velocity. The black box in panel (b) indicates the location of the particle release for the backward-trajectory experiments.
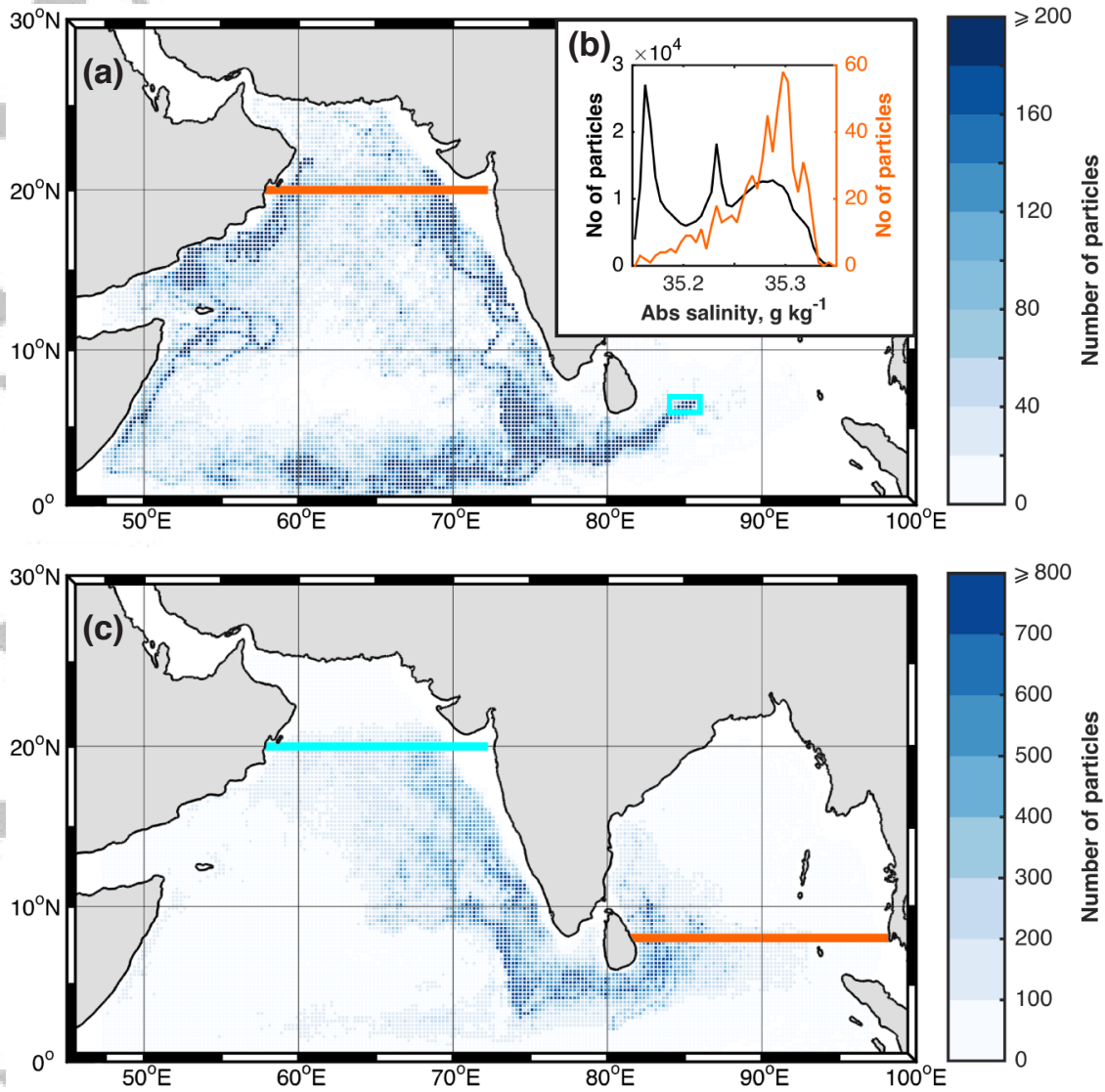
Figure 3. **(a)** Number of particles that pass through quarter-degree latitude-longitude bins during the backward-trajectory experiment. Particles that remain in a bin over consecutive time steps are not counted twice, but particles that enter, exit, then re-enter a bin are counted twice. Only particles that cross 20°N in the northern Arabian Sea (orange line) are included. The release site is enclosed within the light blue box. **(b)** Distribution of the initial salinity (i.e. salinity at release) of particles in the backward-trajectory experiment that do not reach the northern Arabian Sea (black line, left-hand axis) and of particles that do reach the northern Arabian Sea (orange line, right-hand axis). **(c)** As for (a), but for the forward-trajectory experiments, in which particles were released along 20°N in the northern Arabian Sea (light blue line) and tracked forwards in time to 8°N in the BoB (orange line).
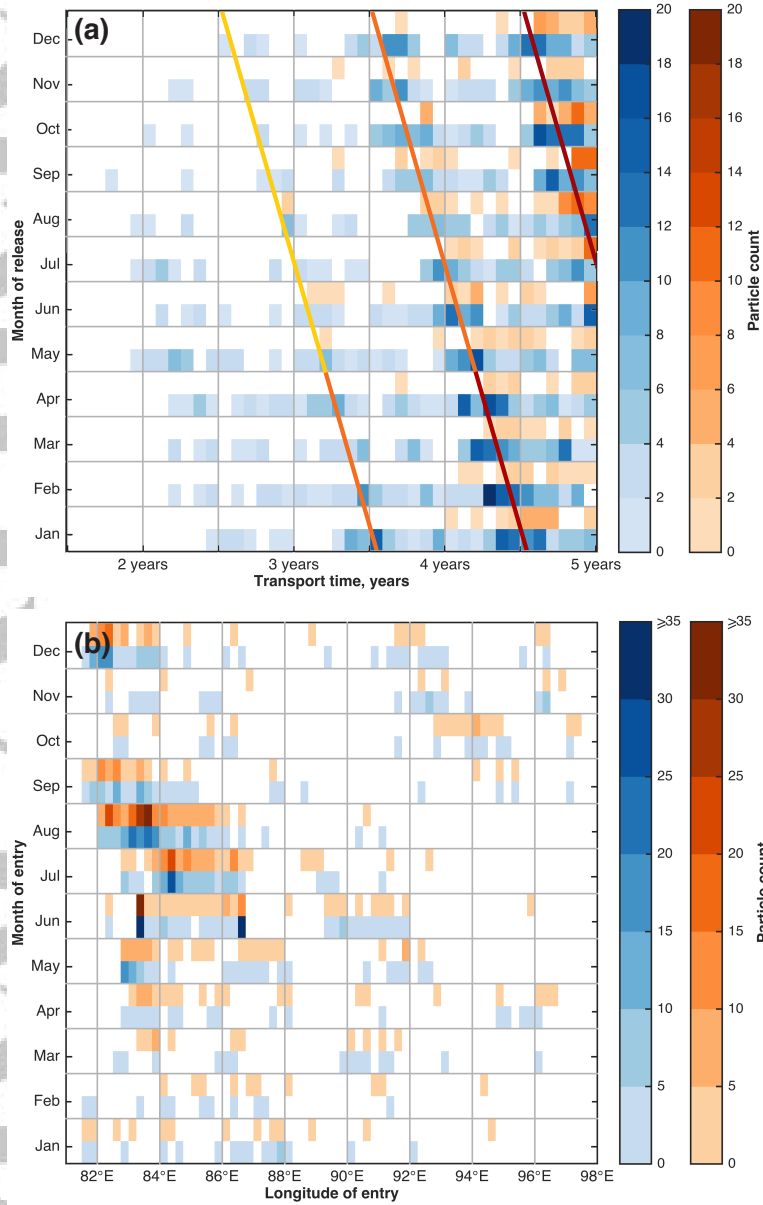
Figure 4. **(a)** The time taken for forwards-tracked particles to reach 8°N in the BoB (one-month bins), by month of release. Particles following the eastern pathway (blue colors) are analysed separately to those following the western pathway (orange colors). The colored lines join transport times that result in particles crossing 8°N in the BoB during the third SW monsoon (yellow), fourth SW monsoon (orange), fifth SW monsoon (red) after release. **(b)** The number of forwards-tracked particles crossing 8°N by month and by longitude (0.25° bins).